Proceedings of the Sixteenth International Conference on
Computational Structures Technology
Edited by: P. Iványi, J. Kruis and B.H.V. Topping
Civil-Comp Conferences, Volume 14, Paper 9.1
Civil-Comp Press, Edinburgh, United Kingdom, 2026
ISSN: 2753-3239, doi: 10.4203/ccc.14.9.1

Bayesian Active Learning of Conditional Failure Probability Distributions for Precast Prestressed Concrete Beams

J. Whiteley and J. Becque

Department of Engineering, University of Cambridge, UK

Abstract

The lateral-torsional buckling of long-span precast prestressed concrete beams during lifting is sensitive to imperfections. This paper investigates the probability of lateral instability given uncertainties in cross-section parameters, material properties and member imperfections. Conditional failure probabilities are investigated, where a measurement of the elastic modulus is taken prior to lifting, and it is researched how such a measurement can be exploited to aid in the assessment of the lateral instability risk. A beam finite element model is combined with a reliability framework, in which the correlation between elastic modulus and tensile strength is captured through a bivariate lognormal distribution. To alleviate the computational cost, a Bayesian active learning strategy is applied to the estimation of conditional response distributions. The method is shown to improve the accuracy of estimates of conditional distributions relative to the use of conventional Gaussian process surrogates.

Keywords: lateral-torsional buckling, precast prestressed concrete beams, Gaussian process surrogate, Bayesian active learning, probability distribution estimation, beam finite element analysis

1 Introduction

The lateral stability of long-span precast prestressed concrete beams is known to be sensitive to the effects of initial imperfections [1]. Of particular importance are the temporary design cases of transportation, lifting on site and placement onto elastic bearings, before the beam's top flange is restrained against lateral movement by the permanent works. In these instances, imperfections arise primarily from differences in the prestressing forces between strands, dimensional tolerances due to formwork placement and shrinkage, and variations in the strength and elastic modulus within the concrete [1]. Such variability lends itself to a probabilistic analysis, given that a worst-case deterministic analysis could be unduly conservative. A stochastic model is formulated in this study, with the aim of characterising the geometric and material uncertainties inherent to precast prestressed concrete girders.

Given a probabilistic model of a structure's performance, a practically relevant question for designers is whether the structural response is sensitive to a reduction or increase in uncertainty in a certain parameter or group of parameters. This notion is explored in the present study through the example of a long-span precast prestressed concrete girder in a hanging configuration. Particular attention is given to the effect of reducing uncertainty in the elastic modulus. The concrete tensile strength and the elastic modulus display a certain degree of correlation (as both are known to depend on the concrete compressive strength). Therefore, the distribution of the tensile strength conditioned on a particular value of the elastic modulus can be obtained through a model of correlation between the two variables. This is useful when, for instance due to project specific constraints, test results, such as from an ultrasonic pulse velocity test, are available for the elastic modulus but not for the tensile strength. Other uncertainties which influence the design, such as geometric imperfections arising from the manufacturing process, are not considered reducible; it is assumed they would be more costly to reduce relative to the uncertainties associated with the material properties.

Evaluating the behaviour of complex structures typically involves the use of finite element analysis. The cumulative computational cost of the many thousands of evaluations needed for sampling-based reliability assessment can thereby become prohibitive. This burden may be alleviated by replacing a finite element model with a machine learning surrogate, such as a Gaussian process [2, 3], trained on a relatively small set of numerical model runs. However, the number of model evaluations required to train a sufficiently accurate surrogate can still be significant, and so active learning strategies are commonly employed [2, 3]. These approaches sequentially select the most informative training points by exploiting a surrogate model's internal probabilistic representation. Such strategies are well established for failure probability estimation, and recent work has extended them to the estimation of entire response distributions [4]. Estimating conditional distributions, in which the response is predicted given partial knowledge of some subset of the input parameters, remains underexplored. This is precisely the setting that arises when a cheaply measured quantity is available and one wishes to update the predictive response distribution conditional on that observation.

In this study, the active learning strategy proposed in [4] is applied to the task of conditional response distribution estimation, through the practically motivated example of a hanging girder susceptible to lateral instability. The suitability of the framework for this new setting is assessed empirically, providing a clear direction for future research in this area.

2 Methods

2.1 Numerical model of lateral stability

2.1.1 Stability design of hanging beams

The lateral stability of long-span precast prestressed concrete beams has been studied extensively by Stratford and Burgoyne [1, 5, 6]. When a beam with an initial lateral sweep v_0 is loaded by its self-weight w per unit length, the additional lateral displacement at midspan, due to the effects of the initial imperfection v_0, is given by the Southwell construction [7]:

$$v = \frac{v_0 \left(1 - \sin \frac{\pi a}{L}\right)}{1 - w/w_{\mathrm{cr}}} \tag{1}$$

where L is the span, a is the overhang from the yoke attachment point to the beam end, and w_{cr} is the critical self-weight per unit length at which lateral buckling occurs. Note that $v_{\mathrm{total}} = v_0 + v$, and that only the additional sweep v, not the initial sweep v_0, is assumed to induce stresses. Figure 1 shows a typical girder arrangement. In the present study, beams are suspended without overhang ($a = 0$). The self-weight per unit length is $w = A\rho g$, where A is the cross-sectional area and $\rho = 2400\ \mathrm{kg/m^3}$ is the density of concrete. The total longitudinal stress at midspan at a fibre located at coordinates (y, z) from the centroid is:

$$\sigma = f_{\mathrm{ps}} - E\kappa y + \frac{M_y}{I_y} z \tag{2}$$

where $M = wL^2/8$ is the midspan moment under self-weight, f_{ps} is the prestress, which is taken negative, and κ is the additional minor-axis curvature caused by the self-weight. Assuming, with some small error, that both the initial and buckled deflected shapes are sinusoidal, then the curvature can be evaluated using:

$$\kappa = \frac{v_0\, \pi^2}{L^2} \cdot \frac{w/w_{\mathrm{cr}}}{1 - w/w_{\mathrm{cr}}} \tag{3}$$

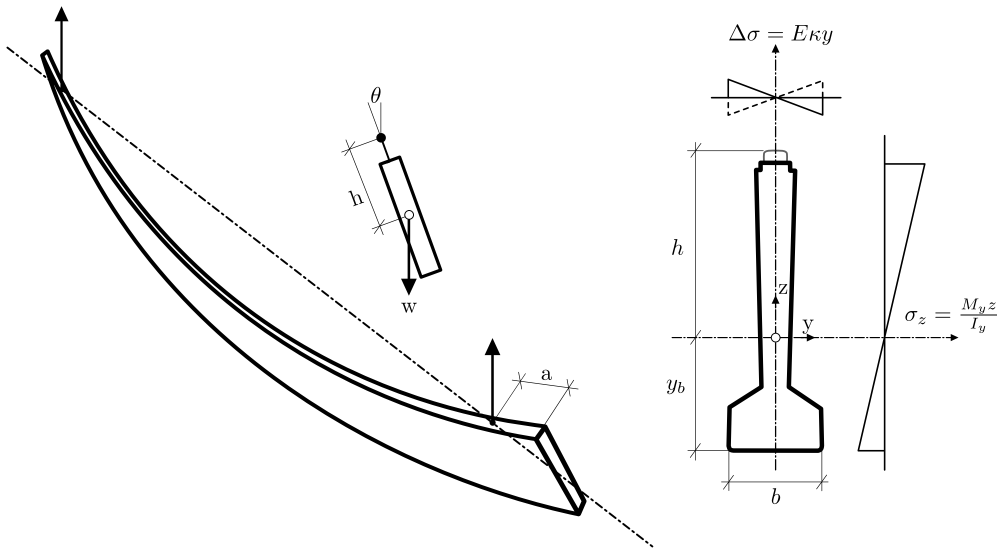

Figure 1: A longitudinal view of a beam's deformed shape with a simplified rectangular cross-section (adapted from [8]); a SY-6 beam cross-section geometry and bending stress distribution (adapted from [1]). Note that the minor axis stresses can have either sign.

2.1.2 Critical buckling load via finite element analysis

The critical buckling load w_{cr} can be obtained from a linear buckling analysis assuming an elastic material. A one-dimensional beam finite element formulation following [9] is used in the present study for this purpose. The formulation employs nodes with seven degrees of freedom $[u_x,\, u_{\bar{y}},\, u_{\bar{z}},\, \theta_x,\, \theta_{\bar{y}},\, \theta_{\bar{z}},\, \phi_x]$, defined relative to the shear centre (y_0, z_0), representing translations and rotations relative to the three axes, in addition to the final entry $\phi_x = \theta'_x$, which captures warping. The incremental potential energy $\Delta U = \Delta U_1 + \Delta U_0 - \Delta W$ separates into elastic strain energy, a geometric stiffness contribution from the initial stress state σ_0, and external work, where:

$$\sigma_0 = \frac{P_0}{A} - \frac{M_{z,0}}{I_z} y + \frac{M_{y,0}}{I_y} z \tag{4}$$

Substituting Hermitian shape functions yields the standard discretisation $\mathbf{K}^*\mathbf{q}^* = \mathbf{F}^*$, where the tangent stiffness matrix $\mathbf{K}^*$ combines elastic and geometric contributions:

$$\Delta U_1 = \int_x \left\{ \tfrac{1}{2} EA\, u_x'^2 + \tfrac{1}{2} EI_z\, u_{\bar{y}}''^2 + \tfrac{1}{2} EI_y\, u_{\bar{z}}''^2 + \tfrac{1}{2} GJ\, \theta_x'^2 \right\} dx \tag{5}$$

$$\Delta U_0 = \int_x \Bigg\{ P_0 \Big[u'_x + \tfrac{1}{2}\, u'^2_{\bar{y}} + \tfrac{1}{2}\, u'^2_{\bar{z}} + \tfrac{1}{2}\, r^2\, \theta'^2_x + z_0\, u'_{\bar{y}}\, \theta'_x - y_0\, u'_{\bar{z}}\, \theta'_x \Big] - M_{y,0} \Big[u''_{\bar{z}} - \beta_z\, \theta'^2_x + u'_{\bar{y}}\, \theta'_x \Big] + M_{z,0} \Big[u''_{\bar{y}} - \beta_y\, \theta'^2_x - u'_{\bar{z}}\, \theta'_x \Big] \Bigg\}\, dx \tag{6}$$

where $r^2 = y_0^2 + z_0^2 + (I_y + I_z)/A$, β_y and β_z, are standard cross-sectional parameters [9]. Warping effects are neglected in Equations 5 and 6 since for typical prestressed concrete beam sections, the contribution of warping restraint to lateral stability is negligible [1]. The resulting stiffness matrix terms are given in the appendix of [9]. While hanging beams lack full torsional restraint at the supports, a restoring moment is provided by the lifting cables, which can be represented by a rotational spring on the θ_x degree of freedom at each support node, with stiffness $k_\theta = w_{\text{cr}} L h/2$. The variable h is the height above the beam centroid of the attachment point (Figure 1). Since k_θ itself depends on w_{cr}, an eigenvalue problem of the form $|\,\mathbf{K}_e - \lambda\, \mathbf{K}_g\,| = 0$ needs to be solved for a few iterations until convergence. The geometric stiffness matrix $\mathbf{K}_g$ is assembled from the reference internal force state $[P_0, M_{y,0}, M_{z,0}]$ corresponding to uniform downwards loading. The critical self-weight is then $w_{\text{cr}} = \lambda_{\text{cr}}\, w$.

2.2 Probabilistic model of imperfect precast prestressed beams

2.2.1 Distributions of the basic random variables

The probabilistic model described in this section characterises the geometric and material uncertainties relevant in the case of hanging precast prestressed concrete girders. Six random variables are considered, summarised in Table 1. The concrete elastic modulus E and tensile strength f_{ct} are modelled following the JCSS Probabilistic Model Code [10], which relates both to the compressive strength f_c via $E_c = 10.5\, f_c^{1/3}$ GPa and $f_{ct} = 0.3\, f_c^{2/3}$ MPa, each with a lognormal distribution and coefficients of variation (CoV) of 0.15 and 0.30, respectively. A correlation of $\rho_{E,f_{ct}}$ is adopted (see Section 2.2.2) to reflect their shared dependence on f_c. The second moments of area, I_y and I_z, are assigned a CoV derived from the JCSS dimensional tolerance model ($\sigma_{X-X_{\text{nom}}} = 4 + 0.006\, X_{\text{nom}}$ mm) propagated through the section geometry. The prestress f_{ps} at the time of lifting has low variability, as jacking forces are tightly controlled and early-age losses are small [14].

The initial lateral sweep v_0 is a critical but poorly characterised parameter. The PCI tolerance [11] is $L/960$, yet measured values show considerable scatter: de la Fuente et al. [12] reported $L/510$ on a girder that failed during lifting, and Hurff [13] measured $L/609$ on a 30 m BT-54-type beam before testing. In the absence of a consensus probabilistic model, a lognormal distribution with mean $L/1000$ [1] and CoV of 0.20 is adopted. The remaining deterministic parameters used in the present study, related to the SY-6 girder referenced in [1], are given in Table 2.

Table 1: Marginal distributions of the basic random variables.

Variable	Distribution	Mean	Unit	CoV	Correlation	Reference
E	Lognormal	34	GPa	0.15	$\rho_{E,f_{ct}} = 0.1$	[10]
f_{ct}	Lognormal	3.5	MPa	0.30	$\rho_{E,f_{ct}} = 0.1$	[10]
I_y	Lognormal	0.2837	m^4	0.05	—	[1, 10]
I_z	Lognormal	0.014	m^4	0.05	—	[1, 10]
v_0	Lognormal	$L/1000$	m	0.20	—	[11–13]
f_{ps}	Lognormal	5	MPa	0.04	—	[14]

2.2.2 Correlation between elastic modulus and tensile strength

The JCSS models for elastic modulus and tensile strength share a common random parameter, f_c, and this gives rise to a correlation between the two quantities. Taking the logarithm of the JCSS relations $E_c = 10.5\, f_c^{1/3}\, Y_3$ and $f_{ct} = 0.3\, f_c^{2/3}\, Y_2$ yields the two expressions:

$$\ln E_c = \ln(10.5) + \tfrac{1}{3} \ln f_c + \ln Y_3 \tag{7}$$

$$\ln f_{ct} = \ln(0.3) + \tfrac{2}{3} \ln f_c + \ln Y_2 \tag{8}$$

where Y_2 and Y_3 are unit-mean lognormal model uncertainty factors (with a CoV of 0.30 and 0.15, respectively). These factors capture scatter from sources not explained by f_c, such as aggregate type and cement chemistry, and they are assumed to be independent of f_c and of each other. Given this, the covariance between the two variables is simply $\mathrm{Cov}(\ln E_c, \ln f_c) = 2/9 \cdot \mathrm{Var}(\ln f_c)$, and hence the correlation between the two is

$$\rho_{\ln E_c, \ln f_{ct}} = \frac{\frac{2}{9}\ \mathrm{Var}(\ln f_c)}{\sqrt{\left[\frac{1}{9}\ \mathrm{Var}(\ln f_c) + \mathrm{Var}(\ln Y_3)\right]\ \left[\frac{4}{9}\ \mathrm{Var}(\ln f_c) + \mathrm{Var}(\ln Y_2)\right]}}. \tag{9}$$

Adopting a CoV of 0.15 for the concrete compressive strength and using the relation $\mathrm{Var}(\ln Y) = \ln(1 + \mathrm{CoV}[Y]^2)$ yields $\mathrm{Var}(\ln f_c) = 0.022$, $\mathrm{Var}(\ln Y_2) = 0.086$ and $\mathrm{Var}(\ln Y_3) = 0.022$, from which $\rho \approx 0.10$.

2.2.3 Conditional distribution of correlated lognormals

The correlation between parameters E and f_{ct} means that learning information about one informs the other. In the scenario when some particular value of the elastic modulus is provided, the conditional distribution of f_{ct} given E is sought. Consider the normally distributed variables Q_1 and Q_2, where $Q_1 = \ln E \sim \mathcal{N}(\mu_E, \sigma_E^2)$ and $Q_2 = \ln f_{ct} \sim \mathcal{N}(\mu_f, \sigma_f^2)$, with correlation ρ between them. These can be expressed as $Q_1 = \mu_E + \sigma_E Z_1$ and $Q_2 = \mu_f + \sigma_f(\rho\, Z_1 + \sqrt{1-\rho^2}\, Z_2)$, where $Z_1, Z_2 \sim \mathcal{N}(0,1)$ are independent. The term Z_1 can be written as $(Q_1 - \mu_E)/\sigma_E$, giving

$$Q_2 = \mu_f + \frac{\rho\, \sigma_f}{\sigma_E}(Q_1 - \mu_E) + \sigma_f \sqrt{1-\rho^2}\, Z_2. \tag{10}$$

Table 2: SY-6 beam parameters [1].

Parameter	Value	Unit	Description
L	32	m	Span
d	2.0	m	Section depth
b	0.75	m	Section width
A	0.709	m^2	Cross-sectional area
J	0.0221	m^4	Torsion constant
y_b	0.855	m	Centroid height above soffit
h	1.6	m	Cable attachment height above centroid
G	14.8	GPa	Shear modulus

The first two terms are deterministic, given Q_1. Conditioning on $Q_1 = q_1$ therefore leaves only Z_2 as the source of randomness, so $Q_2 \mid Q_1{=}q_1 \;\sim\; \mathcal{N}\big(\mu_f + \rho\,\sigma_f\,(q_1 - \mu_E)/\sigma_E,\;\; \sigma_f^2(1-\rho^2)\big)$. Exponentiating, $f_{ct} \mid E{=}E_n$ is lognormal with the stated mean and variance expressions evaluated at $q_1 = \ln E_n$.

2.2.4 Response distribution

Let $Y = g(\mathbf{X})$ be the scalar response obtained by evaluating the limit state function g at the random input $\mathbf{X}$. Figure 2 compares the unconditional CDF $F_Y(y) = P(g(\mathbf{X}) \leq y)$ and PDF $f_Y(y) = \mathrm{d}F_Y/\mathrm{d}y$ of the limit state with their counterparts obtained by conditioning on a particular value of the elastic modulus. Note that $\mathbf{X} = [E, f_{ct}, I_y, I_z, v_0, f_{ps}]$ and that the limit state is given by

$$g(\mathbf{X}) = \sigma(E, I_y, I_z, v_0, f_{ps}) - f_{ct} \tag{11}$$

where σ is given by Equation 2, computed at the bottom corner of the cross-section where tension is maximised, and which takes as an input the curvature $\kappa(w_{cr})$, requiring a critical buckling load w_{cr} computed via finite element analysis. The curves in Figure 2 are obtained by drawing 10^6 Monte Carlo samples of $\mathbf{X}$, either from the unconditional joint distribution $f_{\mathbf{X}}$, or from the conditional distribution $f_{\mathbf{X}|E}$ in which E is fixed and f_{ct} is drawn from the lognormal derived above, with the remaining variables I_y, I_z, v_0, f_{ps} sampled from their marginals since they are independent of E in the model. The limit state $g(\mathbf{X})$ is evaluated for each sample. The PDF is obtained via a Gaussian kernel density estimate of the resulting responses, while the CDF is the empirical CDF of the same samples.

2.3 Bayesian active learning of response distributions

While the Monte Carlo sampling approach utilised in Section 2.2.4 is tractable with the linear finite element analysis formulation applied in this study, it would be prohibitively expensive when using a nonlinear solver. This motivates the use of surrogate models, which, as mentioned, benefit from active learning approaches for the sake of

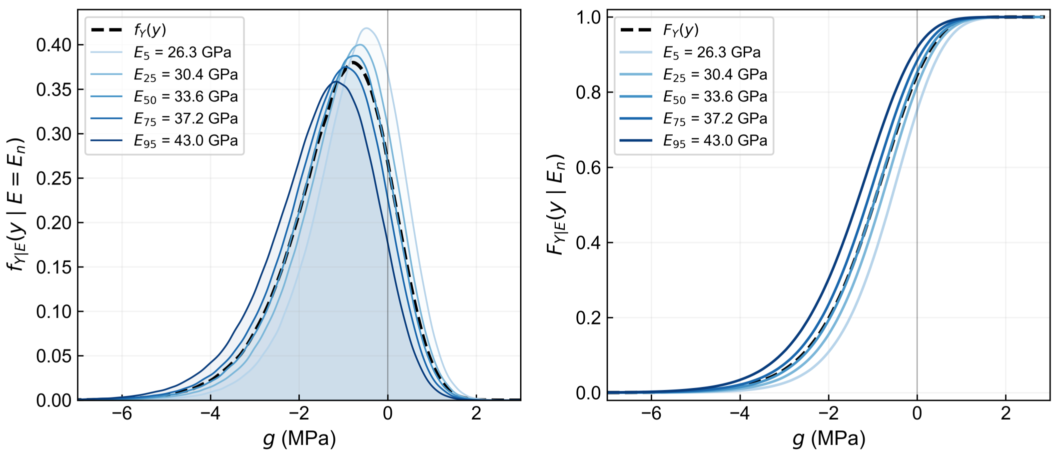

Figure 2: Unconditional and conditional PDFs (left) and CDFs (right) of the limit state g given $E = E_n$, ranging from its 5% to 95% percentile value.

efficiency. Active learning strategies for Gaussian process surrogates in structural reliability have received considerable attention in recent years, however the majority of existing methods target the limit-state surface $g(\mathbf{x}) = 0$ [2]. In the present study, the response CDF is sought instead, following the Bayesian active learning (BAL) framework of [4]. The motivation is twofold: first, the CDF provides the failure probability at any threshold of interest, beyond the typical case $F_Y(0)$; second, it is desired to investigate whether a surrogate that accurately represents $F_Y(y)$ across all thresholds y also provides a reasonable estimate of the conditional CDF $F_{Y|E}(y \mid E = E_n)$.

2.3.1 Gaussian process modelling and posterior CDF estimate

A zero-mean Gaussian process prior with a Matérn-5/2 kernel is placed on g, and after n noiseless observations $\mathcal{D}_n = \{(\mathbf{x}^{(i)}, y^{(i)})\}_{i=1}^n$, the posterior is given by $g_n(\mathbf{x}) \sim \mathcal{GP}(m_{g_n}(\mathbf{x}),\, k_{g_n}(\mathbf{x}, \mathbf{x}'))$, with posterior mean m_{g_n} and standard deviation σ_{g_n} [2]. The uncertainty in g propagates through a chain of transformations to induce a posterior distribution on $F_Y(y)$ [4]. First, the indicator function $I_A(\mathbf{x}) = \mathbf{1}[g(\mathbf{x}) \leq y]$ inherits a posterior from g_n, with mean:

$$m_{I_A,n}(\mathbf{x}) = \Phi\left(\frac{y - m_{g_n}(\mathbf{x})}{\sigma_{g_n}(\mathbf{x})}\right). \tag{12}$$

The response CDF $F_Y(y) = \int I_A(\mathbf{x})\, f_{\mathbf{X}}(\mathbf{x})\, \mathrm{d}\mathbf{x}$ then inherits, via integration, a posterior with mean:

$$m_{F_Y,n}(y) = \int \Phi\left(\frac{y - m_{g_n}(\mathbf{x})}{\sigma_{g_n}(\mathbf{x})}\right) f_{\mathbf{X}}(\mathbf{x})\, \mathrm{d}\mathbf{x}, \tag{13}$$

with an analogous expression $m_{\bar{F}_Y,n}(y)$ for the complementary CDF (CCDF) obtained by replacing $\Phi(z)$ with $\Phi(-z)$. The posterior variance of $F_Y(y)$ involves a double integral over the covariance kernel of I_A and is computationally demanding. Instead, an upper bound is obtained as [4]:

$$\bar{\sigma}_{F_Y,n}(y) = \int \sqrt{\Phi\left(\frac{y - m_{g_n}(\mathbf{x})}{\sigma_{g_n}(\mathbf{x})}\right)\, \Phi\left(\frac{-(y - m_{g_n}(\mathbf{x}))}{\sigma_{g_n}(\mathbf{x})}\right)}\, f_{\mathbf{X}}(\mathbf{x})\,\mathrm{d}\mathbf{x}. \tag{14}$$

All integrals above can be evaluated numerically via Monte Carlo sampling, following the estimators given in [4].

2.3.2 Two-step acquisition function

The accuracy of the response distributions can be quantified by the upper-bound coefficient of variation $H_n(y) = \max\big(\overline{\mathrm{CoV}}_{F_Y,n}(y),\ \overline{\mathrm{CoV}}_{\bar{F}_Y,n}(y)\big)$, where the term $\overline{\mathrm{CoV}}_{F_Y,n} = \bar{\sigma}_{F_Y,n}/m_{F_Y,n}$ and likewise for the CCDF. This expression provides a principled means of determining whether the surrogate has been trained on a sufficient quantity of data; the quantity $\max_y H_n(y) < \epsilon$ for some threshold ϵ is a natural stopping criteria. When the stopping criterion is not met, an additional training point can be selected in two steps. First, the response level to target is identified using

$$y^\star = \arg\max_y\ H_n(y). \tag{15}$$

The next evaluation point can then be chosen by maximising a learning function over the input space:

$$\mathbf{x}^{(n+1)} = \arg\max_{\mathbf{x}}\ \sqrt{\Phi\left(\frac{y^\star - m_{g_n}(\mathbf{x})}{\sigma_{g_n}(\mathbf{x})}\right)\Phi\left(\frac{-(y^\star - m_{g_n}(\mathbf{x}))}{\sigma_{g_n}(\mathbf{x})}\right)}\ f_{\mathbf{X}}(\mathbf{x}) \tag{16}$$

The learning function is the integrand of $\bar{\sigma}_{F_Y,n}(y^\star)$ in Equation (14), so it quantifies the contribution of each input location $\mathbf{x}$ to the total posterior uncertainty of the CDF at the most uncertain response level. In practice, the $f_{\mathbf{X}}$ weighting is handled implicitly by evaluating the expression over a candidate pool drawn from $f_{\mathbf{X}}$, and the maximisation in Equation (15) is performed over a discrete grid of y values.

3 Results

Figure 3 shows unconditional and conditional response distributions estimated by both a Gaussian process model trained by randomly sampling from $\mathbf{X} \sim f_{\mathbf{X}}$ and a model trained with the BAL framework described in the preceding section. In the latter case, 10 initial random samples were taken, before adding 15 additional samples with BAL. Monte Carlo reference solutions are also provided based on 10^6 random samples. For both the CDF and CCDF, the BAL-trained model tracks the reference tails of the unconditional distributions significantly better than the randomly trained surrogate, particularly where probabilities drop below approximately 10^{-2}, which is typically the region of interest for the reliability analysis of structures. This divergence

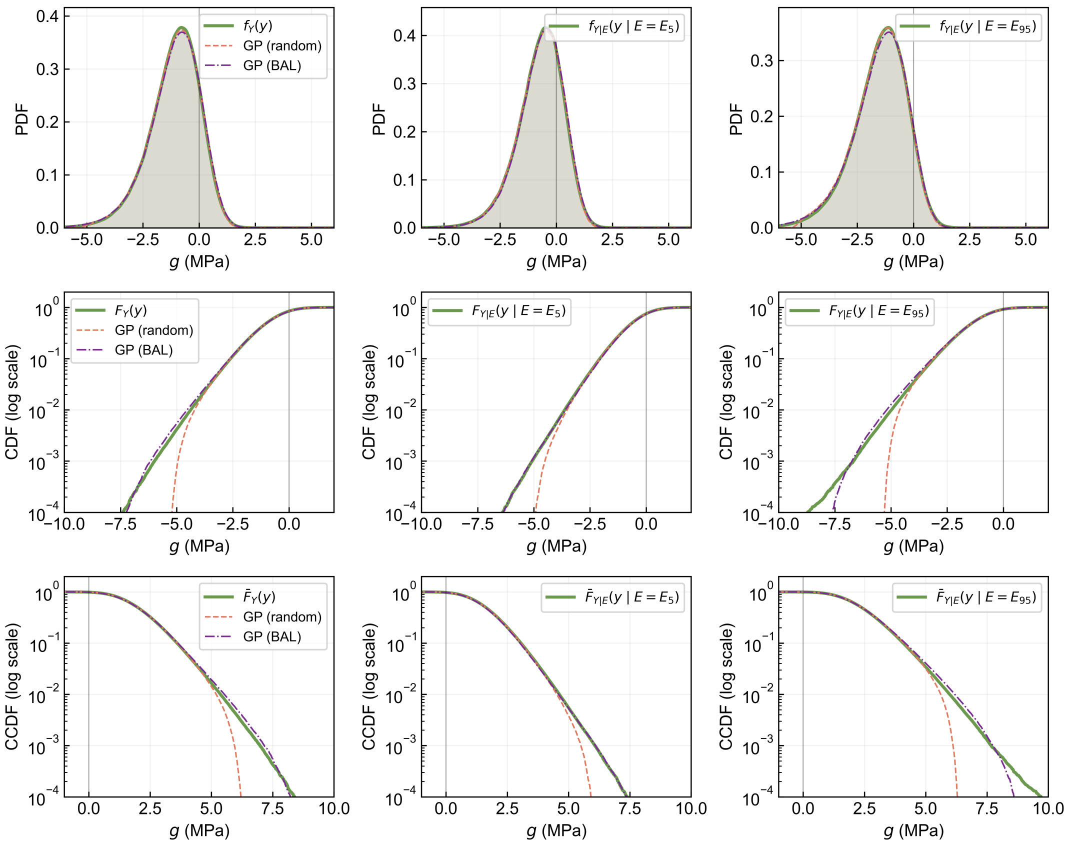

Figure 3: Response PDF (top), CDF (middle) and CCDF (bottom) for the unconditional distribution (left), conditional on $E = E_5$ (centre) and conditional on $E = E_{95}$ (right). The BAL-trained Gaussian process captures the tails of the CDF and CCDF more accurately than the randomly trained Gaussian process, despite the fact that both are only trained on 25 data points.

in performance between the two models is expected, as the acquisition function explicitly targets response levels where the coefficient of variation of the CDF or CCDF is largest, concentrating training points in the tails. In the PDF plots, the difference between the two approaches is not noticeable.

The BAL-trained Gaussian process estimates for the conditional distributions are also improved relative to the randomly trained surrogate. This suggests that the unconditional BAL strategy transfers with reasonable accuracy to the conditional case. However, the performance for the conditional cases is degraded somewhat, and this provides an impetus for further investigations in modified acquisition functions specifically for the case of conditional response distribution estimation.

4 Conclusions and contributions

This study has investigated the applicability of a Bayesian active learning strategy, originally developed for unconditional response distribution estimation, to the task of estimating conditional response distributions. The framework was assessed through the practically motivated example of a hanging precast prestressed girder susceptible to lateral instability, in which the response distribution of interest is conditioned on an observation of the concrete's elastic modulus.

The results show that Gaussian process surrogates trained via the unconditional BAL strategy yield conditional distribution estimates that are noticeably improved relative to those obtained from randomly trained surrogates. Performance in the conditional case is, however, degraded compared with the unconditional case, which motivates the development of new acquisition functions tailored specifically to conditional response distribution estimation.

Beyond the methodological contribution, the application itself is of practical relevance. The spread of the conditional failure probability across observed values of elastic modulus quantifies how much a measurement of the material stiffness prior to lifting would reduce uncertainty in the assessed risk of lateral instability, providing a basis for downstream decision-theoretic analyses [15] of whether such testing is worthwhile.

References

[1] T.J. Stratford, C.J. Burgoyne, H.P.J. Taylor, "Stability design of long precast concrete beams", *Proceedings of the Institution of Civil Engineers – Structures and Buildings*, 134(2), 159–168, 1999.

[2] B. Echard, N. Gayton, M. Lemaire, "AK-MCS: An active learning reliability method combining Kriging and Monte Carlo simulation", *Structural Safety*, 33(2), 145–154, 2011.

[3] J. Whiteley, J. Becque, "A Bayesian optimization approach for reliability-based design of prestressed concrete structures", *Data-Centric Engineering*, 7(3), 2026.

[4] C. Dang, M.A. Valdebenito, N.A. Manque, J. Xu, M.G.R. Faes, "Response probability distribution estimation of expensive computer simulators: A Bayesian active learning perspective using Gaussian process regression", *Structural Safety*, 114, 102579, 2025.

[5] T.J. Stratford, C.J. Burgoyne, "Lateral stability of long precast concrete beams", *Proceedings of the Institution of Civil Engineers – Structures and Buildings*, 124(2), 169–180, 1999.

[6] T.J. Stratford, C.J. Burgoyne, "The toppling of hanging beams", *International Journal of Solids and Structures*, 37(26), 3569–3589, 2000.

[7] R.V. Southwell, "On the analysis of experimental observations in problems of elastic stability", *Proceedings of the Royal Society of London. Series A*, 135(828), 601–616, 1932.

[8] R.F. Mast, "Lateral stability of long prestressed concrete beams – Part 1", *PCI Journal*, 34(1), 1989.

[9] Z.P. Bažant, M. El Nimeiri, "Large-deflection spatial buckling of thin-walled beams and frames", *Journal of the Engineering Mechanics Division*, 99(6), 1259–1281, 1973.

[10] JCSS, "Probabilistic Model Code, Part 3: Resistance Models", *Joint Committee of Structural Safety*, 2000. Available at: `https://www.jcss-lc.org`.

[11] PCI Plant Certification Committee et al., *Manual for Quality Control for Plants and Production of Structural Precast Concrete Products*, Precast/Prestressed Concrete Institute, 1999.

[12] A. De la Fuente, J.M. Bairán, S.H.P. Cavalaro, "Case study of failure of long prestressed precast concrete girder during lifting", *Engineering Failure Analysis*, 100, 512–519, 2019.

[13] J.B. Hurff, L.F. Kahn, "Rollover stability of precast, prestressed concrete bridge girders with flexible bearings", *PCI Journal*, 57(4), 2012.

[14] A.S. Nowak, M.M. Szerszen, "Calibration of Resistance Factors for the Design of Concrete Structures", in: *Proc. International Symposium on High Performance Computing*, Tokyo, 2003.

[15] D. Straub, M. Ehre, I. Papaioannou, "Decision-theoretic reliability sensitivity", *Reliability Engineering & System Safety*, 221, 108215, 2022.